# Fatigue-resistant epitaxial Pb(Zr,Ti)03 capacitors on Pt electrode with ultra-thin SrTi03 template layers



doi: 10.1016/j.tsf.2008.04.078

# Fatigue-resistant epitaxial $Pb(Zr,Ti)O_3$ capacitors on Pt electrode with ultra-thin $SrTiO_3$ template layers

Seiichi Takahara[a,1], Akiharu Morimoto[a,*], Takeshi Kawae[a], Minoru Kumeda[a], Satoru Yamada[b], Shigeru Ohtsubo[b], and Yasuto Yonezawa[c]

[a] *Div. of Electrical Eng. and Computer Sci., Graduate School of Natural Sci. and Technol., Kanazawa University, Kakuma-machi, Kanazawa 920-1192, Japan*

[b] *Department of Electronic Engineering, Ishikawa National College of Technology, Tsubata 929-0392, Japan*

[c] *Industrial Research Institute of Ishikawa, Kanazawa 920-0223, Japan*

(Received )

Lead zirconate-titanate $Pb(Zr,Ti)O_3$ (PZT) capacitors with Pt bottom electrodes were prepared on MgO substrates by pulsed laser deposition (PLD) technique employing $SrTiO_3$ (STO) template layer. Perovskite PZT thin films are prepared via stoichiometric target using the ultra-thin STO template layers while it is quite difficult

[1] Present address: Kanazawa Murata Mfg., Co., Ltd., Hakusan 920-2101, Japan

[*] Corresponding author: e-mail amorimot@ec.t.kanazawa-u.ac.jp, tel +81-76-234-4876

to obtain the perovskite PZT on Pt electrode via stoichiometric target in PLD process. The PZT capacitor prepared with the STO template layer showed good hysteresis and leakage current characteristics, and it showed an excellent fatigue-resistance. The ultra-thin STO template layers were characterized by angle-resolved X-ray photoelectron spectroscopy measurement. The effect of the STO template layer is discussed based on the viewpoint of the perovskite nucleation and diffusion of Pb and O atoms.

Key words:

Ferroelectric properties; Lead zirconate-titanate (PZT); Pulsed laser deposition (PLD); Strontium Titanate (STO)

## 1. Introduction

Ferroelectric random access memory (FeRAM) is well known as one of the promising candidates for nonvolatile RAM because of the low power operation, the high speed, and the structural similarity to the dynamic RAM. However, the FeRAM has crucial problems to be solved, for instance, on polarization fatigue, imprint and retention[1]. Lead zirconate titanate Pb(Zr, Ti)$O_3$ (PZT) thin films have been employed for the FeRAM application owing to the high remnant polarization and low processing temperature. The FeRAM reliability issues such as the polarization fatigue, imprint *etc*., however, are closely related not only to bulk properties of PZT films but also to their electrodes and the interface structures. Then, a variety of preparation methods have been applied for the fabrication of PZT capacitors on various electrodes, and the problems, *e.g.,* the polarization fatigue, imprint[2], retention[3, 4] and low integration density[5] were analyzed and overcome to some extent. Recently, Lou *et al*. proposed a fatigue mechanism that PZT thin films on Pt electrode undergo a local phase decomposition from perovskite to pyrochlore phase during the polarization fatigue[6]. Further efforts on the basic study are required for the PZT application to the reliable and high density FeRAM.

PZT is well known to have two crystal phases, *i.e*., the perovskite phase (high

temperature phase) with ferroelectric property and the pyrochlore phase (low temperature phase) with paraelectric property. In addition, high temperature fabrication often causes another pyrochlore phase due to deficiency of Pb[7-9]. Namely, the ferroelectric perovskite phase has two limits on both the low and high temperature sides. The temperature region between the two limits can be denoted by *perovskite window*. A precise control of the preparation condition is essential for the fabrication of the ferroelectric perovskite phase. Especially on Pt electrode, it is quite difficult to obtain the perovskite phase by pulsed laser deposition (PLD) because of a Pb deficiency on Pt electrode due to a low sticking coefficient of Pb or a diffusion of Pb into the electrode. The obstacles have been overcome by supplying excess Pb during preparation compared with the stoichiometric composition[10,11]. In the fabrication process, however, usage of excess Pb is undesirable from the viewpoint of cross contamination problems because the excess Pb must be evaporated in the preparation chamber. Furthermore, the basic understanding of the stability of the interface structure between stoichiometric PZT and Pt electrode is also crucial for reliable device fabrication.

In 1990, we reported that perovskite PZT films were prepared on various substrates by PLD[12]. Then we prepared perovskite PZT films on Ni-alloy and Ti-Al-N electrodes[13,14]. Then, the PLD methods have attracted much attention in the field of

ferroelectrics as a useful method to prepare good films. The most outstanding advantage is the stoichiometric transfer of material from a target to a substrate, resulting in the stoichiometric film composition without any special technique. Therefore, the above-mentioned failure in getting perovskite PZT films on Pt by PLD seems to be coming from the unique PLD feature of stoichiometric source flux supply. Obtaining the perovskite PZT films on Pt electrode via stoichiometric source material is quite important for clarifying the growth mechanism of perovskite PZT films on Pt.

In addition, Pt electrode has another problem on the polarization fatigue of PZT capacitors. Nowadays, this problem has been partly solved by employing oxide electrodes owing to the elimination of oxygen deficiency at the PZT and Pt interface during the polarization switching[15,16]. Without using oxide electrode, it is still difficult to obtain fatigue-free PZT capacitors on pure Pt electrode.

In the present study, excellent perovskite PZT films were fabricated on Pt electrodes by PLD employing a $SrTiO_3$ (STO) ultra-thin template layer between PZT and Pt layers. STO thin film was introduced by PLD using $SrTiO_3$ ceramic target. Since STO has the perovskite structure with a lattice constant of 0.3905 nm, single crystal STO has been widely used as a substrate for some perovskite oxide films such as PZT. In addition, the voltage drop in the STO layer of the applied voltage should be small

because of its high dielectric constant[17,18]. So far, there is no report on STO template layer for the PZT film deposition although there have been many reports on the $PbTiO_3$ template layer for the perovskite PZT film[19-21]. Kwok and Desu reported that 45 nm-thick PT layer expanded the *perovskite window*[22]. The STO template layer, however, is expected to be superior as a template layer because of the Pb-free nature. The Pb-free STO growth does not require special care on the preparation condition for preventing the Pb desorption; especially, the oxygen pressure and substrate temperature. In this paper we report that nearly fatigue-free PZT capacitors with excellent ferroelectric properties were obtained on Pt electrodes employing a STO template layer and we discuss the growth mechanism of PZT films on Pt based on the results obtained by the angle-resolved x-ray photoelectron spectroscopy (ARXPS)[23].

**2. Experiment**

PZT films were prepared by PLD. To fabricate the capacitor structure, first of all, the Pt bottom electrodes were deposited epitaxially on single crystal (100)MgO substrates using PLD method with a repetition frequency of 10 Hz at a temperature of 600˚C in vacuum. The MgO substrates were cared for avoiding deliquescence before loading into the chamber. The Pt film thickness was about 100 nm, and in-plane

epitaxial relationship was found to be [100] Pt // [100] MgO by means of X-ray pole figure measurement, *i.e.*, the cube-on-cube epitaxy. STO films for template or buffer layers were prepared by the PLD using $SrTiO_3$ ceramic target at a temperature of 700˚C in an oxygen pressure of 0.13 Pa. The deposition conditions of PZT films are summarized in Table I. The top electrodes were fabricated by thermal evaporation of Au using metal shadow mask with $3.14\times10^{-4}$ $cm^2$ in area size unless otherwise noted.

The surface microstructure and crystallographic orientation of PZT films were characterized by means of scanning electron microscopy (SEM) with an acceleration voltage of 20 kV and x-ray diffraction (XRD), respectively. The XRD measurement with Cu $K_\alpha$ radiation consists of θ-2θ scan, θ-scan (rocking curve) and pole figure measurement. The ferroelectric characteristics (P-E hysteresis) were evaluated by an RT-66A ferroelectric test system (Radiant Technologies) at virtual ground mode. The fatigue characteristics were also examined by the RT-66A using rectangular bipolar pulses with a frequency of 100 kHz and a voltage of 12 V. The thin STO layers were characterized by means of ARXPS.[23]

**3. Results and discussion**

Figure 1 shows the XRD patterns of PZT films deposited at 600˚C in oxygen of

13 and 40 Pa on the Pt/MgO with or without thin STO layer. The thin STO layers were deposited on Pt/MgO substrates at 700˚C in oxygen of 0.13 Pa before the PZT deposition. In case where PZT film was deposited directly on the Pt/MgO substrate, almost no perovskite PZT phase was observed, resulting in the predominant pyrochlore phase in the XRD pattern. This result indicates that deficiency of Pb or O[8,9] atoms from the stoichiometry occurs during the initial nucleation process of PZT film because of the stoichiometric target employed. However, the pyrochlore phase disappeared completely by introducing a thin STO layer (10 shots) into the PZT/Pt interface, and the perovskite PZT became dominant and the [001]-axis strongly oriented along the film plane normal. These results suggest that a thin STO layer plays a dual role of diffusion barrier of Pb or O and template layer for the nucleation of perovskite PZT. The resultant PZT/STO/Pt/MgO structure was confirmed to have epitaxial relationship, or cube-on-cube epitaxy, by the X-ray pole figure measurement. The surface SEM photographs of the perovskite PZT film deposited at 600˚C in oxygen of 40 Pa on Pt/MgO using thin STO layer indicated that the PZT film is very dense with several tens nm grains.

From the above results, the insertion of the thin STO layer into the PZT/Pt interface is found to be effective for obtaining perovskite PZT film in PLD process. It is

quite important to understand the reason why those results were obtained. To clarify this point, the STO thickness dependence of the crystal structure of PZT films was examined. Figure 2 shows the XRD patterns of PZT films for various film thicknesses of the STO layer. No perovskite PZT phase was observed in the XRD pattern for the sample without a STO layer in the PZT/Pt interface. However, when the STO layer was inserted by two laser shots at the interface, the perovskite phase slightly appeared in addition to the pyrochlore phase. When it was prepared by four laser shots, the pyrochlore phase disappeared completely and the PZT turned to the perovskite single phase. The film thickness for four laser shots was calculated to be 0.5 nm which is obtained from the slope of the thickness vs. shot plot. This thickness is approximately equivalent to one unit cell of the perovskite STO.

It is difficult to understand the role of STO sufficiently just based on the above discussion on the average film thickness. Can we expect the above effect, if the Pt bottom electrode is not fully covered by the STO layer? Thus, an ARXPS measurement was performed in order to investigate whether the STO film shows 3- dimensional (3D or island) growth or 2- dimensional (2D) growth. This ARXPS measurement was performed by changing the angle of the XPS detector against the film surface and measuring the intensity of signals from the atoms close to the surface and atoms below

them as shown in Fig.3. The ARXPS measurement is one of the powerful techniques for investigating the surface state of ultra thin films without sample destruction[23]. The STO sample prepared by four laser shots on Pt film was used for ARXPS measurement. This sample is the thinnest one among the samples that showed the perovskite enhancement effect as shown in Fig. 2. The normalized intensity of the underneath Pt signal against the Sr signal in the STO layer, $I_{norm}(\theta)$, was derived experimentally and theoretically as shown in Fig. 4.

In general, the photoelectron intensity of A atoms as a function of the take-off angle $i^{A}(\theta)$ can be calculated by the following equation,

$$i^{A}(\theta) = C^{A} \exp\left( -\frac{x}{\lambda^{A} \sin\theta} \right) \qquad (1) .$$

Here, $C^{A}$, $x$ and $\lambda^{A}$ are a cross section of photoelectrons of A atoms, the depth of A atoms and the escape depth of photoelectrons of A atom, respectively. The angle θ is the take-off angle from the film surface as shown in Fig.3. Based on Eq.(1), the following equation can be derived by integrating the total photoelectron intensity of Sr atoms $I^{Sr}(\theta)$ over $0 < x < d_{STO}$ in the STO layer and integrating the total photoelectron intensity of Pt atoms $I^{Pt}(\theta)$ over $d_{STO} < x <$ infinity in the Pt layer. $I^{Pt}(90)$ and $I^{STO}(90)$ are the intensities of respective photoelectrons at θ=90 ˚.

$$I_{norm}(\theta)=\frac{\frac{I^{Pt}(\theta)}{I^{Pt}(90)}}{\frac{I^{Sr}(\theta)}{I^{Sr}(90)}}=\frac{\exp\left(-\frac{d_{STO}}{\lambda^{Pt}}\left[\frac{1}{\sin\theta}-1\right]\right)}{\frac{\left\{1-\exp\left(-\frac{d_{STO}}{\lambda^{Sr}\sin\theta}\right)\right\}}{\left\{1-\exp\left(-\frac{d_{STO}}{\lambda^{Sr}}\right)\right\}}} \qquad (2)$$

Here, $d_{STO}$, $\lambda^{Pt}$, and $\lambda^{Sr}$ are the depth of the STO/Pt interface layer measured from the STO surface (the thickness of the thin STO layer), the escape depth of Pt4f photoelectrons ($\lambda^{Pt}$ =2.219 nm), and the escape depth of Sr3d photoelectrons ($\lambda^{Sr}$ =2.125 nm), respectively. These escape depths are assumed to be determined only by the kinetic energy of the respective photoelectrons, not by the kind of matrix. The angle dependence of the photoelectron excitation was cancelled out by the normalization procedure described in Eq.(2). In short, the normalization of the measured angle-resolved signal intensity of Pt4f by that of Sr3d was performed in order to remove influence of the instrumental angle-dependent excitation. The normalization by the respective intensities at 90 ° was performed in order to remove the cross section of photoelectrons of respective atoms.

Figure 4 shows the $\ln(I_{norm}(\theta))$ vs $1/\sin\theta$ plots of the ARXPS data and the calculated value using Eq. (2). For comparison, the results of normalizations using C1s and O1s signals are also presented because those C atoms possibly locate on almost the topmost surface of the STO thin layer and O atoms locate within the STO thin layer.

Irrespective of the method of normalization, there is no big difference in the observed values among them. If 2-D STO exists on the Pt layer, the escape distance of Pt4f photoelectrons will become large as the take-off angle becomes small. Therefore, the signal intensity of Pt4f photoelectrons decreases rapidly based on Eq. (2). On the other hand, if the STO is in an island-like growth mode, the angle dependence of the signal intensity of Pt4f photoelectron will become weak and the plot will show a saturation behavior. In Fig. 4, all of the plots show similar behavior as Eq. (2) irrespective of the way of normalization. These results suggest that the STO layer is the ultra-thin 2D film. It is interesting that thin film deposited by PLD has 2D growth mode while cluster or droplets depositions are often observed in PLD process. The 2D growth appears to originate from the surface migration enhanced by high-energy depositing particles.

The theoretical line drawn using Eq. (2) with the STO thickness of 0.8 nm agrees well with the experimental data. This value is lager than the value of 0.5 nm estimated from the deposition rate. The discrepancy between them can be ascribed to the well-known large ambiguity of the escape depths or ambiguity of the film thickness estimated from the deposition rate because the initial growth rate may be different from the steady-state-growth rate. In the following discussion, for the sake of simplicity, we use the values estimated from the deposition rate as the thickness of the STO layers.

In any case, these results on the structural analysis suggest that the effect of thin STO layer originates from the template effect for the perovskite nucleation rather than the effect of diffusion barrier. Layer with thickness of 1 nm or below cannot play a crucial role in diffusion barrier but can play a crucial role for the perovskite nucleation. For better electrical properties, thicker template around 5 or 10 nm, however, was used while the structural measurements revealed that thin template with 1 nm or less was sufficient for obtaining the perovskite.

Figure 5 shows the *P-E* hysteresis loop of Au/PZT(300 nm)/STO(5 nm)/Pt/MgO capacitor. A good hysteresis loop is obtained for both the oxygen pressures, and no bad influence of the STO is seen. The remnant polarization $2P_r$ and the coercive field $2E_c$ of the PZT film prepared in the oxygen pressure of 40 Pa were 59.8 μC/cm$^2$ and 151.5 kV/cm, respectively, while those of the PZT film prepared in the oxygen pressure of 13 Pa were 25.4 μC/cm$^2$ and 117.2 kV/cm, respectively. The degradation of $2P_r$ for the PZT film prepared in the oxygen pressure of 13 Pa seems to be caused by deficiency of oxygen. The leakage current for both the PZT samples was found to be below $10^{-5}$ A/cm$^2$ around 200 kV/cm.

Figure 6 shows the fatigue characteristics of the Pt/PZT(500 nm)/STO(10 nm)/Pt/MgO capacitor. The PZT film was prepared at 600˚C in the oxygen pressure of

40 Pa. For long-term characterization of the fatigue resistance Pt top electrode is preferable due to the mechanical toughness while for short time electrical measurements Au top electrode is sufficient. The 200 nm-thick Pt top electrode was fabricated using metal shadow mask with $3.14\times10^{-4}$ $cm^2$ in area size by PLD in vacuum at room temperature. Then, the sample was annealed at 600˚C for 30 min in an oxygen pressure of 1 atm in order to remove damage induced by high energy Pt atom deposition. Generally, a rapid $P_r$ decrease around $10^6$~$10^8$ cycles was reported when Pt is used as a bottom electrode[24] because Pb or O atoms diffuse through grain boundary of Pt electrode. However, even after $10^{11}$ switching cycles ΔP for the present sample keeps the value above 80 % of the initial ΔP even if the sample just employs Pt top and bottom electrodes. These results suggest that the STO layer stabilize the PZT/Pt interface leading to the improved fatigue characteristic.

Based on the recent fatigue model for Pt/PZT/Pt capacitors proposed by Lou *et al*.[6], the present improvement of fatigue resistance can be ascribed to the suppression of the phase change from the perovskite to pyrochlore phase. They showed that PZT thin films undergo local phase decomposition during fatigue. The original remnant polarization of the fatigued film is completely restored after furnace annealing in an oxygen atmosphere, as a result of regrowth of a perovskite phase from the pyrochlore

structure[6]. In the present films, a stable stoichiometric PZT/STO/Pt interface may suppress the phase change, resulting in the fatigue resistant capacitor. It should be noted that the improvement has been attained only by modification of bottom interface in the present study. The capacitors has still top Pt/PZT interface. This asymmetric effect suggests that the polarization fatigue of PZT capacitors with Pt electrode seems to originate from the bottom interface. This idea differs from the idea of Lou *et al*. based on the importance of top electrode. In the present electrical characterization, we cannot completely deny the role of STO buffer layer for suppressing the Pb or O diffusion similarly to the oxide electrodes, because the sample for electrical measurements were prepared with 5 nm thick STO, thicker than 1 nm thick STO layer for XRD and ARXPS measurements. The high dielectric oxide is found to show a crucial role in the fatigue resistance, similarly to oxide electrodes. This effect is ascribed to the common feature of two materials; the structural stability and the low voltage loss in the capacitor.

**4. Conclusions**

We prepared PZT thin films on Pt/MgO by PLD technique using an STO template layer, and investigated the effect of the STO template layer on the structure and properties of PZT. Perovskite PZT thin films were prepared even from the

stoichiometric target using the ultra-thin STO template layer. The PZT capacitor prepared with the STO template layer on the bottom Pt electrode shows good electrical characteristics and an excellent fatigue-resistance. These results are originating from the stable PZT/STO/Pt interface.

**Acknowledgements**

The authors would like to thank Prof. Emeritus T. Shimizu of Kanazawa University for helpful discussions. We would like to thank Mr. Y. Kurata of Kanazawa University for technical supports, and also thank Mr. Y. Oshio and Mr. A. Ueki of Kanazawa University for technical assistance. This research was partially supported by Japan Society for the Promotion of Science (JSPS), Grant-in-Aid for Exploratory Research, 15651049, 2003 & 2004.

**References**

[1] J. F. Scott, Ferroelectric Memories, Springer, New York NY, 2000.

[2] P. J. Schorn, P. Gerber, U. Boettger, R. Waser, G. Beitel, N. Nagel, R. Bruchhaus, Integr. Ferroelectr. 73 (2005) 83.

[3] B. J. Bae, J. E. Lim, D. C. Yoo, S. D. Nam, J. E. Heo, D. H. Im, B. O. Cho, S. O. Park, H. S. Kim, U. I. Chung, J. T. Moon, Integr. Ferroelectr. 75 (2005) 235.

[4] S. P. Kim, J. M. Koo, S. M. Shin, Y. S. Park, Appl. Phys. Lett. 87 (2005) 212910.

[5] K. N. Kim, S. Y. Lee, J. Appl. Phys. 100 (2006) 051604.

[6] X. J. Lou, M. Zhang, S. A. T. Redfern, J. F. Scott, Phys. Rev. Lett. 97 (2006) 177601.

[7] E. Sato, Y-H. Huang, M. Kosec, A. Bell, N. Setter, Appl. Phys. Lett. 65 (1994) 2678.

[8] S-O. Chung, J. W. Kim, G. H Kim, C. O. Park, W. J. Lee, Jpn. J. Appl. Phys. 36 (1997) 4386.

[9] S-G. Lee, K-T. Shim, Y-H. Lee, Jpn. J. Appl. Phys. 38 (1999) 217.

[10] T-S. Kim, D-J. Kim, J-K. Lee, H-J. Jung, J. Mater. Res. 13 (1998) 3436.

[11] X. M. Lu, J. S. Zhu, W. S. Hu, Z. G. Liu, Y. N. Wang, Appl. Phys. Lett. 66 (1995) 2481.

[12] S. Otsubo, T. Maeda, T. Minamikawa, Y. Yonezawa, A. Morimoto, T. Shimizu, Jpn. J. Appl. Phys. 29 (1990) L133.

[13] A. Morimoto, Y. Yamanaka, T. Shimizu, Jpn. J. Appl. Phys. 34 (1995) 4108.

[14] A. Morimoto, Y. Yamanaka, T. Shimizu, Jpn. J. Appl. Phys. 35 (1996) L227.

[15] M. Dawber, J. F. Scott, Appl. Phys. Lett. 76 (2000) 1060.

[16] H. Z. Jin, J. Zhu, J. Appl. Phys. 92 (2002) 4594.

[17] S. Komatsu, K. Abe, N. Fukushima, Jpn. J. Appl. Phys. 37 (1998) 5651.

[18] M. Tachiki, M. Noda, K. Yamada, T. Kobayashi, J. Appl. Phys. 83 (1998) 5351.

[19] T.-L. Ren, L.-T. Zhang, L.-T. Liu, Z.-J. Li, Jpn. J. Appl. Phys. 40 (2001) 2363.

[20] T. Sakoda, K. Aoki, Y. Fukuda, Jpn. J. Appl. Phys. 38 (1999) 5162.

[21] K. Ishikawa, K. Sakura, D. Fu, S. Yamada, H. Suzuki and T. Hayashi, Jpn. J. Appl. Phys. 37 (1998) 5128.

[22] C-K. Kwok, S. B. Desu, J. Mater. Res. 8 (1993) 339.

[23] A. Masuda, I. Fukushi, Y. Yonezawa, T. Minamikawa, A. Morimoto, M. Kumeda, T. Shimizu, Jpn. J. Appl. Phys. 32 (1993) 2794.

[24] J. F. Scott, C. A. Araujo, B. M. Melnick, L. D. Mcmillan, R. Zuleeg, J. Appl. Phys. 70 (1991) 382.

## FIGURE CAPTIONS

FIG. 1 XRD patterns of PZT films deposited on Pt/MgO without STO layer(a) and with thin STO(5 nm) layers (b, c). PZT films were prepared at 600˚C in the oxygen pressure of 13 Pa (a, b) and in the oxygen pressure of 40 Pa (c).

FIG. 2 XRD patterns of PZT films for the various thicknesses of the STO layers prepared by PLD with 0 shot (a), 2 shots (b), 4 shots (c), and 10 shots (d).

FIG. 3 Outline of the ARXPS measurement. The ARXPS measurement configuration and magnified sample cross section for the photoelectron intensity calculation.

FIG. 4 $\ln(I_{norm}(\theta))$ vs $1/\sin\theta$ plots of the ARXPS data obtained by experiment and the calculated value using Eq. (2).

FIG. 5 P-E characteristics of Au/PZT(300 nm)/STO(5 nm)/Pt/MgO capacitor. PZT films were prepared at 600˚C in the oxygen pressure of 40 Pa and 13 Pa.

FIG. 6 Fatigue characteristics of the Pt/PZT(500 nm)/STO(10 nm)/Pt/MgO capacitor. The PZT film was prepared at 600˚C in the oxygen pressure of 40 Pa.

**Figure**

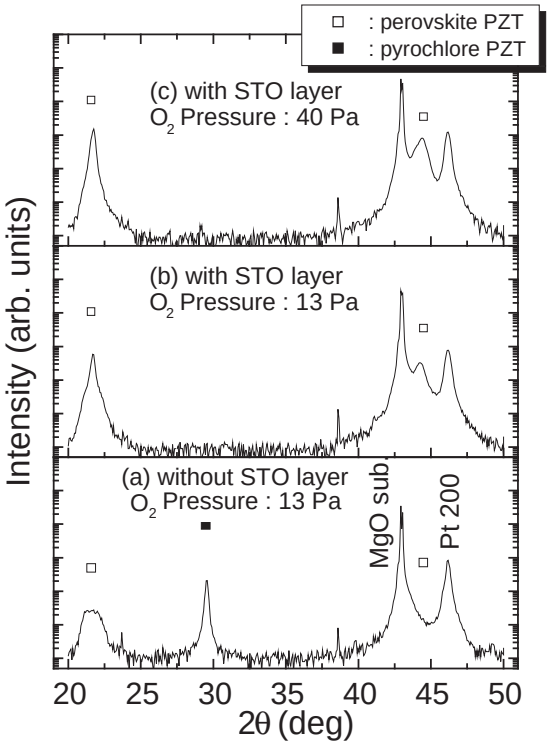
□ : perovskite PZT
■ : pyrochlore PZT
(c) with STO layer
O2 Pressure : 40 Pa
(b) with STO layer
O2 Pressure : 13 Pa
(a) without STO layer
O2 Pressure : 13 Pa
MgO sub.
Pt 200
Intensity (arb. units)
20
25
30
35
40
45
50
2θ (deg)

FIG.1

**Figure**

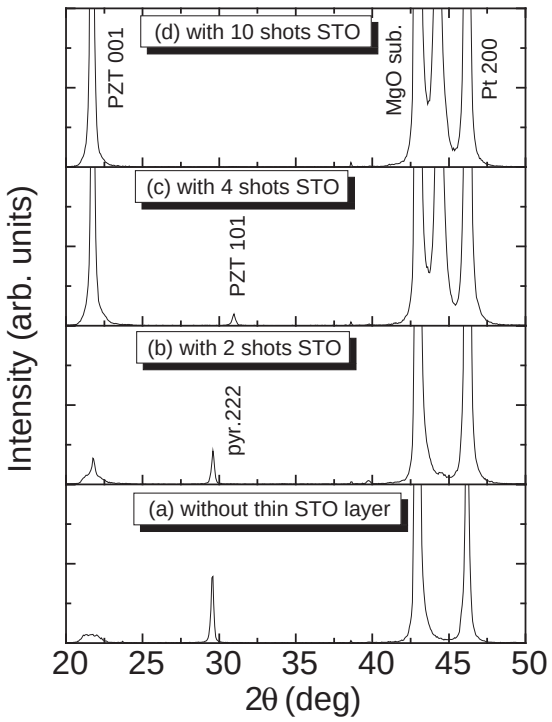
(d) with 10 shots STO
PZT 001
MgO sub.
Pt 200
(c) with 4 shots STO
PZT 101
(b) with 2 shots STO
pyr.222
(a) without thin STO layer
Intensity (arb. units)
20
25
30
35
40
45
50
2θ (deg)

FIG.2

**Figure**

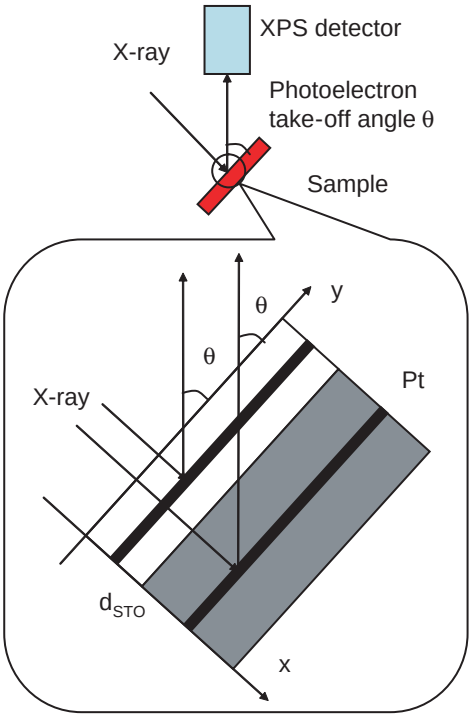
XPS detector
X-ray
Photoelectron
take-off angle θ
Sample
θ
y
θ
Pt
X-ray
$d_{STO}$
x

FIG.3

**Figure**

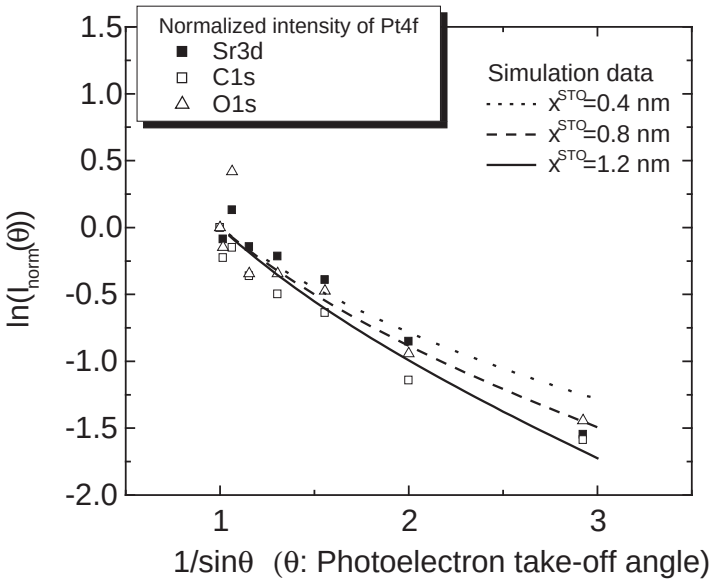
Normalized intensity of Pt4f
Sr3d
C1s
O1s
Simulation data
x^STO=0.4 nm
x^STO=0.8 nm
x^STO=1.2 nm
ln(I_norm(θ))
1.5
1.0
0.5
0.0
-0.5
-1.0
-1.5
-2.0
1
2
3
1/sinθ (θ: Photoelectron take-off angle)

FIG.4

**Figure**

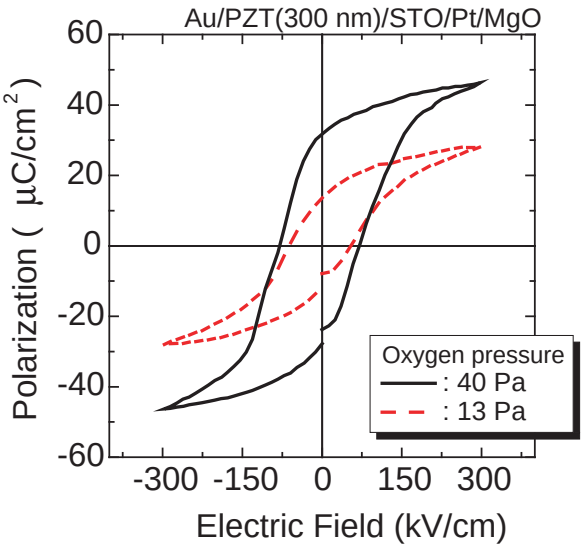
Au/PZT(300 nm)/STO/Pt/MgO
Polarization ( μC/cm$^2$ )
60
40
20
0
-20
-40
-60
-300
-150
0
150
300
Electric Field (kV/cm)
Oxygen pressure
: 40 Pa
: 13 Pa

FIG.5

**Figure**

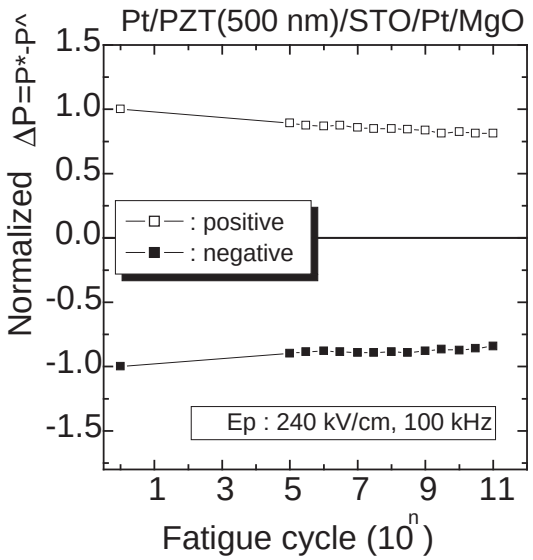
Pt/PZT(500 nm)/STO/Pt/MgO
Normalized ΔP=P*-P^
1.5
1.0
0.5
0.0
-0.5
-1.0
-1.5
: positive
: negative
Ep : 240 kV/cm, 100 kHz
1
3
5
7
9
11
Fatigue cycle (10^n)

FIG.6

**Table**

Table I. Preparation condition of PZT films

| | |
|---|---|
| Laser | KrF excimer laser |
| Wavelength | 248 nm |
| Pulse width | 20 ns |
| Repetition rate | 5 Hz |
| Laser fluence | 2.81 J/cm$^2$ |
| oxygen gas pressure | 40, 13 Pa |
| Substrate temperature | 600 ˚C |
| Substrate | (100)Pt/(100)MgO |
| Target | sintered $Pb(Zr_{0.52}Ti_{0.48})O_3$ target |
| Target-substrate distance | 35 mm |
| PZT film thickness | 300, 500 nm |